Electronic Supplementary Material (ESI) for Chemical Science. This journal is © The Royal Society of Chemistry 2019

**Electronic supporting information**

# Under-liquid Dual Superlyophobic Nanofibrous Polymer Membranes Achieved by Coating Thin-film Composites: A Design Principle

Qifei Wang,[a] Yang Wang,[b] Baixian Wang,[a] Zhiqiang Liang,[a] Jiancheng Di,[*a] and Jihong Yu[*ac]

[a] State Key Laboratory of Inorganic Synthesis and Preparative Chemistry, College of Chemistry, Jilin University, Changchun 130012 (P. R. China)

[b] Department of Mechanical Engineering, City University of Hong Kong, 83th Tat Chee Avenue, Kowloon, Hong Kong

[c] International Center of Future Science, Jilin University, Changchun 130012 (P. R. China)

* Co-corresponding authors

Email: jcdi@jlu.edu.cn, jihong@jlu.edu.cn

**Table of contents in Supporting Information**:


1. Table of contents S2
2. Experimental Section S3
3. Results and discussions S4

1). **Figure S1.** S4

2). **Figure S2.** S5

3). **Figure S3.**. S6

4). **Figure S4.** S7

5). **Figure S5.**. S8

6). **Figure S6.** S9

7). **Figure S7.** S10

8). **Figure S8.** S12

9). **Figure S9.** S13

10). **Figure S10.** S14

11). **Figure S11.** S15

12). **Figure S12.** S16

13). **Table S1.** S17

14). **Table S2.** S18

15). **Table S3.** S19

16). **Table S4.** S21

17). **Table S5.** S23

18). **Table S6.** S23

19). **Table S7.** S24

20). **Table S8.** S25

21). **Table S9.** S26

4. References S27

## Experimental Section

**Materials:** Polyacrylonitrile (PAN, 150,000, 90%) was purchased from the Jilin Chemical Company. Silver nitrate was purchased from Shanghai Shiyi Chemiclas Reagent Company. Dimethylformamide (DMF), nitric acid (65%) and hydrazine dihydrochloride were purchased from Beijing Chemical Company. 1,4-Dicyanobezene (98%), 4-cyanobenzoic acid (99%) and 3-phenylpropiononitrile (99%) were purchased from ACROS Organic Company. 4-(Trifluoromethoxy)benzonitrile (98%), 3-(trifluoromethyl)benzonitrile (98%), 4-hydroxybenzonitrile (99%), Sudan III and Methylene blue were purchased from Aladdin Company. 1-Naphthonitrile (95%) and 4-nitrobenzonitrile (98%) were purchased from TCI Company. 3-Fluoro-4-hydroxybenzonitrile (98%) and 4-fluorophenylacetonitrile (97%) were purchased from ALFA Company. Hydrazine hydrate (50 wt%), hydrofluoric acid (40%) and dimethyl sulfoxide (DMSO) were purchased from Tianjin Fuchen Chemical Company. Ethylene glycol, cyclohexane (CYH), cetane, n-hexane, petroleum ether, tetrachloromethane (TCM), nitromethane and formamide were purchased from Beijing Chemical Company. Silica wafer with 100 orientation was purchased from Suzhou Jingxi Technology Company.

**Results and discussions**

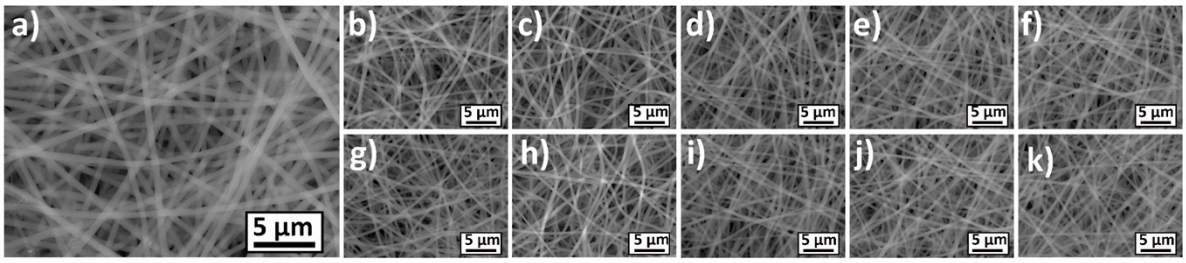


**Figure S1.** Morphologies of PAN nanofibers and TFPNs with different terminal groups. SEM images of a) PAN nanofibers, b) 4-trifluoromethoxy-Ph-terminated TFPNs, c) naphthyl-terminated TFPNs, d) 3-trifluoromethyl-Ph-terminnated TFPNs, e) 4-fluoro-Ph-terminated TFPNs, f) 3-fluoro-4-hydroxy-Ph-terminated TFPNs, g) phenyl-terminated TFPNs, h) 4-nitro-Ph-terminated TFPNs, i) 4-hydroxy-Ph-terminated TFPNs, j) plasma-treated CTFPNs and k) 4-carboxyl-Ph-terminated TFPNs. The similar diameters of these uniform intertwined nanofibers indicate that the further modification process has little effect on the surface geometries.

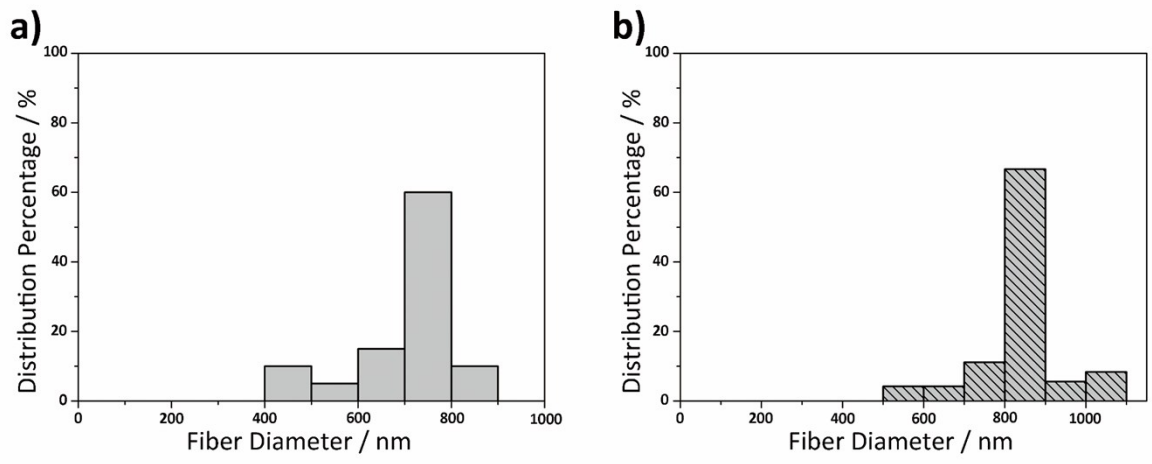


**Figure S2.** Distribution curves of the fiber diameters of a) PAN nanofibers and b) CTFPN.

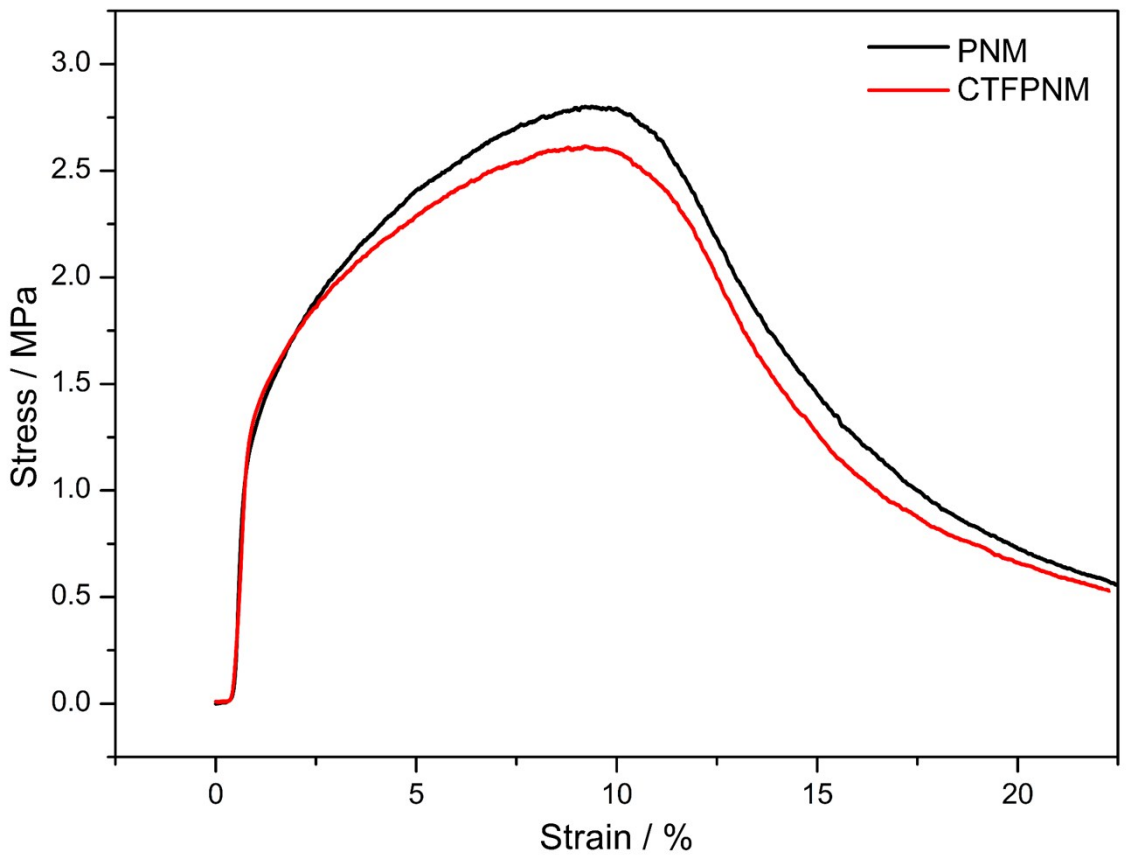


**Figure S3.** The stress-strain curves of PNM and CTFPNM. The derived Young's modulus and stress of break of CTFPNM are 410.1 ± 1.7 and 2.6 ± 0.1 MPa, respectively, which are close to those of PNM (488.0 ± 1.9 and 2.8 ± 0.1 MPa).[1]

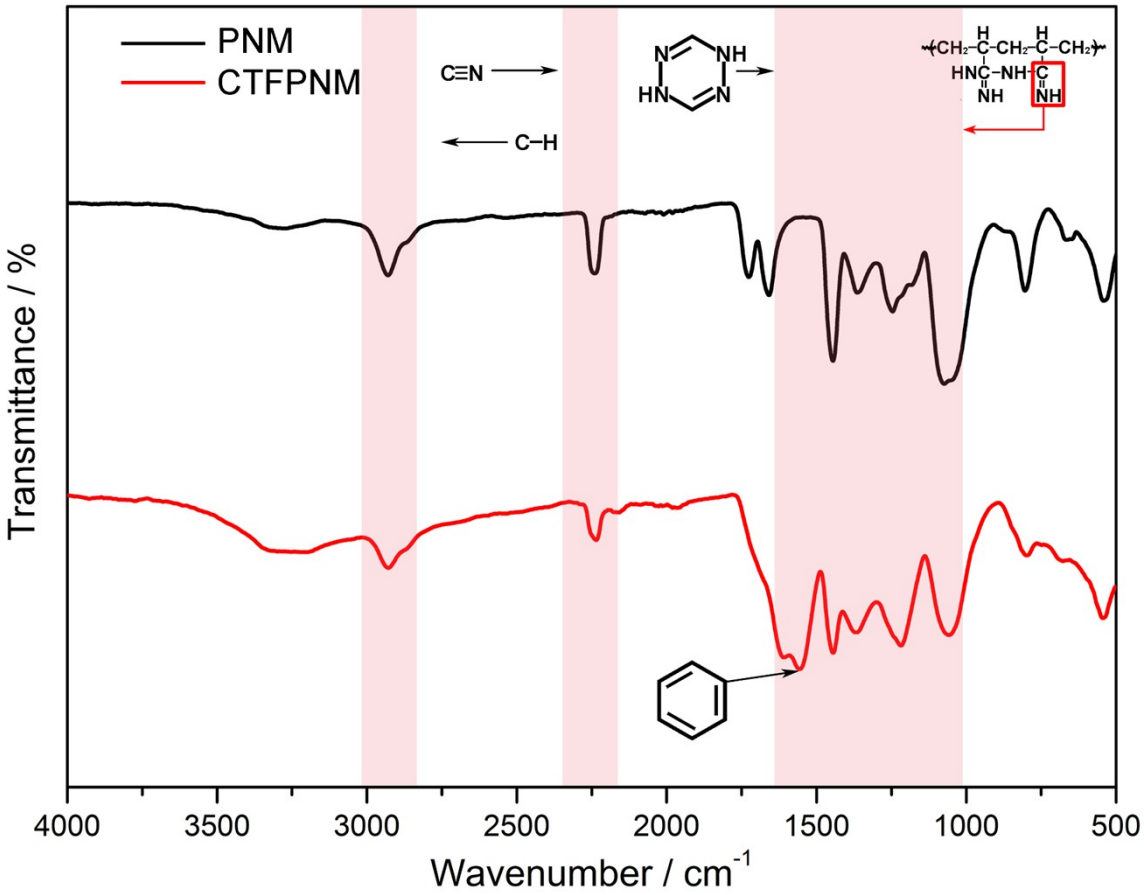


**Figure S4.** FT-IR spectra of the PNM and CTFPNM. The intensity of adsorption peak at 2250 $cm^{-1}$ (C≡N stretching vibration) for CTFPNM decreases, which is attributed to the polymerization between hydrazine hydrate the terminal cyano group.[2] The absorption peak appeared at 1580 $cm^{-1}$ in the spectra of CTFPNM is assigned to the benzene ring.[3] The broad adsorption peak located in the region of 1080-1640 $cm^{-1}$ correspond to the stretching vibrations of C=N (1634 $cm^{-1}$) and N-N (1100 $cm^{-1}$), mixed C-N stretching and N-H bending vibrations (1200-1350 $cm^{-1}$).[2, 4] The other peak in this region (1460 $cm^{-1}$), as well as the peak at 2920 $cm^{-1}$, correspond to the C-H band of alkane groups.[2]

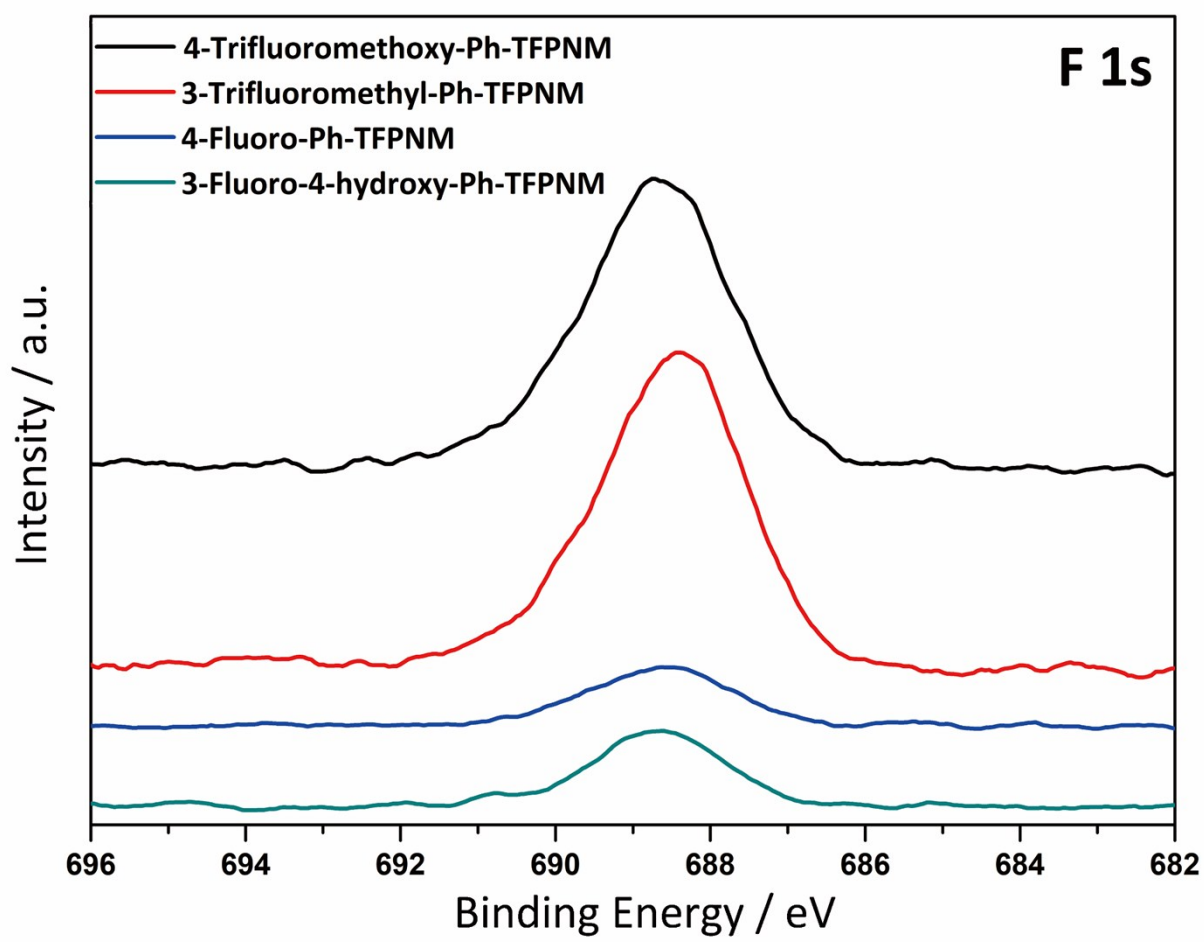


**Figure S5.** XPS spectra of the 4-trifluoromethoxy-Ph-TFPNM, 3-trifluoromethyl-Ph-TFPNM 4-fluoro-Ph-TFPNM and 3-fluoro-4-hydroxy-Ph-TFPNM.

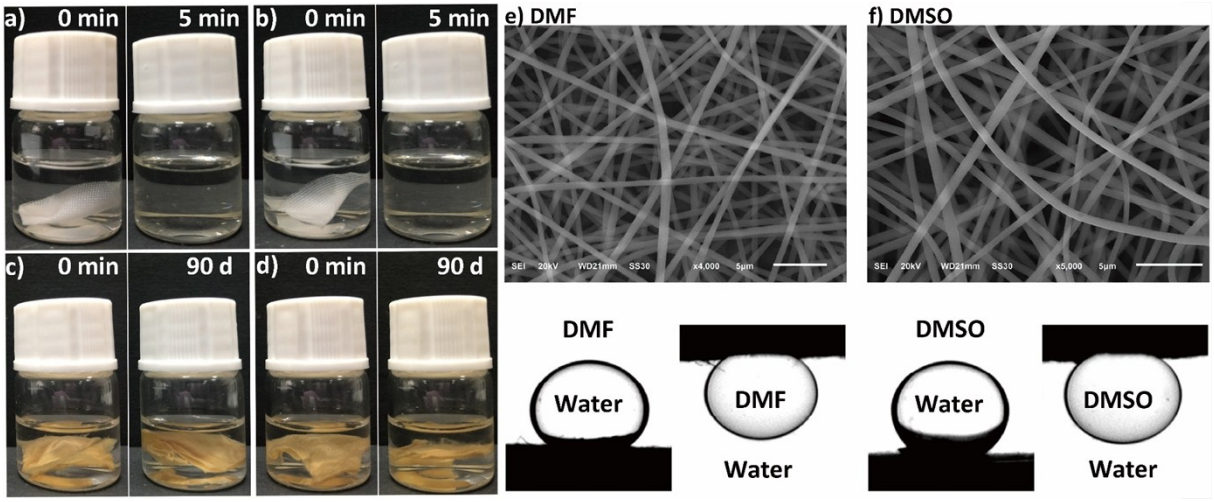


**Figure S6.** Stability tests of CTFPNMs in organic solvents. a) and b) Photographs of PNMs in DMF and DMSO, respectively, in which the membranes are dissolved within 5 min. c)and d) Photographs of CTFPNMs in DMF and DMSO, respectively. The CTFPNMs remain stable after soaking for 90 d. e) and f) The SEM images and the under-liquid wetting behaviors of CTFPNMs after soaking in DMF and DMSO solution for 90 days, respectively, which is similar to that of the fresh-prepared CTFPNM, showing excellent organic solvent stability.

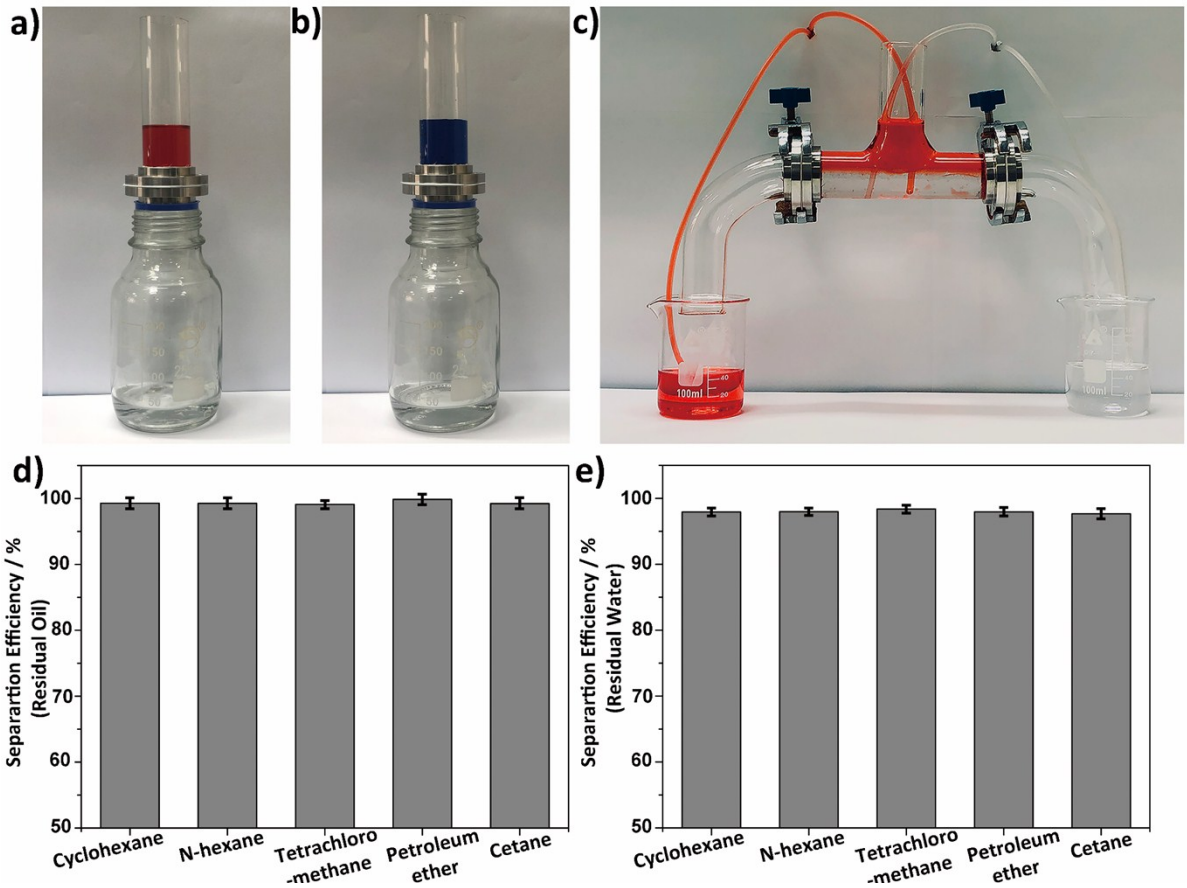


**Figure S7.** The separation of oil/water mixtures. a) The removal of water from CYH/water mixture by water-prewetted CTFPNM (CYH, red liquid, dyed by Sudan III). b) The removal of TCM from TCM/water mixture by TCM-prewetted CTFPNM (water, blue liquid, dyed by Methylene blue). c) Continuous separation of CYH/water mixture. d) and e) The separation efficiencies of CTFPNM for a series of oil/water mixtures, which are calculated by measuring the residual oil content and water content in the filtrates after the continuous separation process for 1 h, respectively.

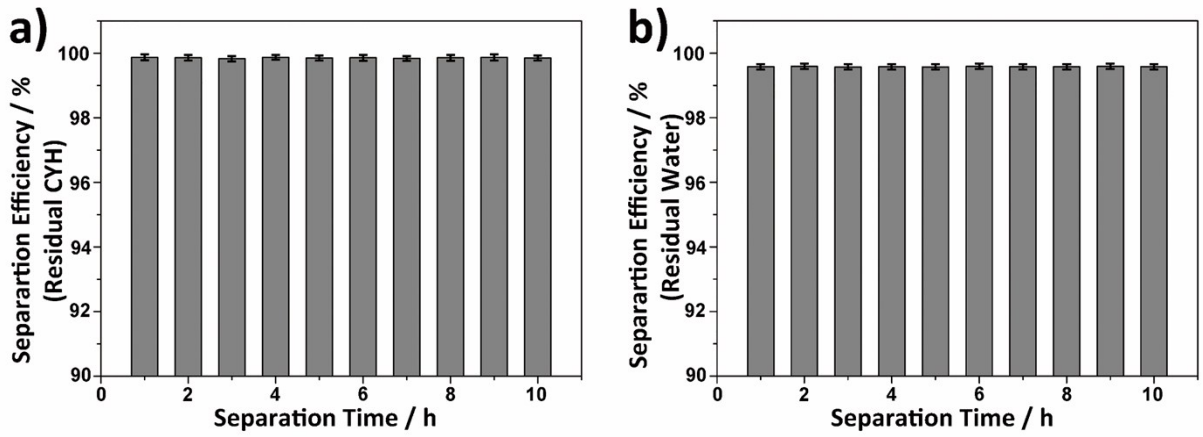


**Figure S8.** Separation stability test of CTFPNM. a) and b) The separation efficiencies of CTFPNM for the water/CYH mixture during the 10 h separation process. The separation efficiencies are calculated by measuring the residual oil content and water content in the filtrates for each hour, respectively, which keep stable and no visible attenuation is observed, proving the high stability of CTFPNM.

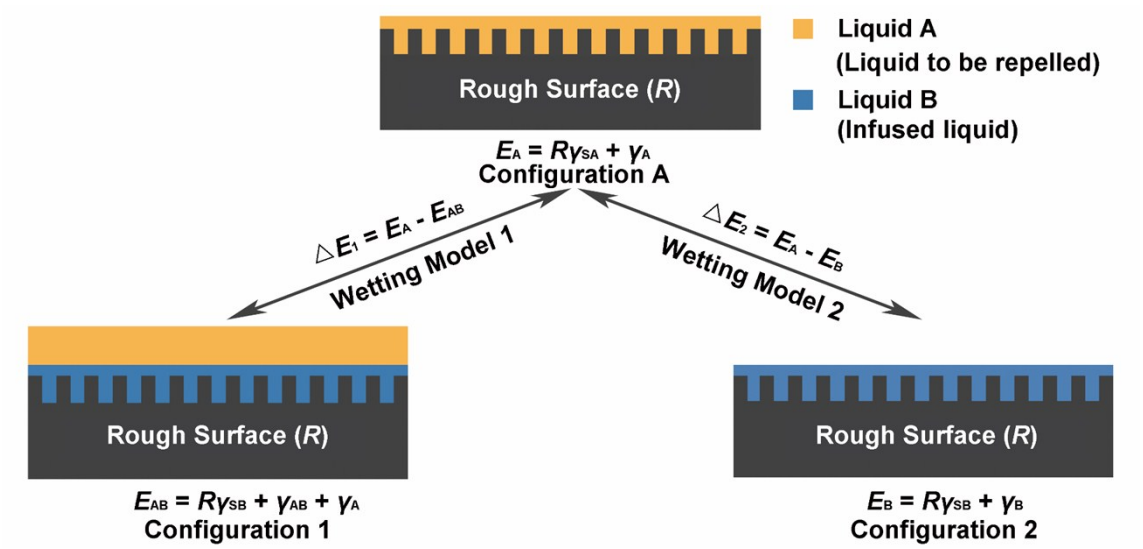


**Figure S9.** Thermodynamic wetting models.[5, 6] Configurations A and 2 represent the states that the solid surface is sufficiently infused by liquid A and B, respectively. Configurations 1 represents the state that the solid surface is previously infused by liquid B and gets liquid A floating on the top.

To determine whether a solid would be wetted preferentially by liquid A or liquid B, the total interfacial energies of the wetting configurations (A, 1, 2) were analyzed. As is known that the preferred wetting state should possess the lower surface energy. Therefore, in the case that the solid surface is preferentially infused by liquid B, we should have $E_A > E_B$ or $E_{AB}$, which can be expressed as,

$$\Delta E_1 = R(\gamma_{SA} - \gamma_{SB}) - \gamma_{AB} > 0 \qquad \text{(S1)}$$

$$\Delta E_2 = R(\gamma_{SA} - \gamma_{SB}) + \gamma_B - \gamma_A > 0 \qquad \text{(S2)}$$

where $\gamma_{SA}$ and $\gamma_{SB}$ represent the surface tensions of the liquid A–solid interface and liquid B–solid interface, respectively. $\gamma_A$ and $\gamma_B$ are the surface tensions of the liquid to be repelled and the infused liquid (Table S6), respectively. $\gamma_{AB}$ represents the surface tension of the liquid A-liquid B interface (Table S7). $R$ is the roughness factor of the solid, which is defined as the ratio of the actual and projected areas of the solid surface.

In particular, the equation S1 and S2 could be reduced to measurable quantities by using the Young's Equation (see equation S3) and be transformed into derivatives (for example, Y. Wang et al., *Nat. Commun*., 2017, **8**, 575 and T. Wong et al., *Nature*, 2011, **477**, 443-447), thus we have,

$$\cos\vartheta = \frac{\gamma_{SV} - \gamma_{SL}}{\gamma_{LV}} \qquad \text{(S3)}$$

$$\Delta E_1 = R[(\gamma_{SV} - \gamma_A\cos\vartheta_A) - (\gamma_{SV} - \gamma_B\cos\vartheta_B)] - \gamma_{AB} > 0 \qquad \text{(S4)}$$

$$\Delta E_2 = R[(\gamma_{SV} - \gamma_A\cos\vartheta_A) - (\gamma_{SV} - \gamma_B\cos\vartheta_B)] + \gamma_A - \gamma_B > 0 \qquad \text{(S5)}$$

where $\gamma_{SV}$, $\vartheta_A$, and $\vartheta_B$ are the surface tension of the solid-vapor interface and where $\vartheta_A$ and $\vartheta_B$ are the intrinsic contact angles of liquid A (the liquid to be repelled) and liquid B (the infused liquid) on the flat solid surfaces (Table S3), respectively.
By further reducing equations (S4 and S5) into a more concise form, we have,

$$\Delta E_1 = R(\gamma_B\cos\vartheta_B - \gamma_A\cos\vartheta_A) - \gamma_{AB} > 0 \qquad \text{(S6)}$$

$$\Delta E_2 = R(\gamma_B\cos\vartheta_B - \gamma_A\cos\vartheta_A) + \gamma_A - \gamma_B > 0 \qquad \text{(S7)}$$

When the calculated results fulfill the the above equations, that is, $\Delta E_1$ and $\Delta E_2$ are all greater than zero, it means that the soild surface is preferentially infused by liquid B, forming a stable liquid B-solid interface to repell the liquid A. Meanwhile, liquid A will be substituted by liquid B from the liquid A-solid interface. In contrast, when both $\Delta E_1$ and $\Delta E_2$ are less than zero, the liquid A-solid interface is more stable and liquid B will be substituted by liquid A from the liquid B-solid interface. When the signs of $\Delta E_1$ and $\Delta E_2$ are opposite, these formulas cannot predict the under-liquid wetting behaviors of surfaces. Different soild surfaces have been explored by the equations above with oil and water, respectively (Table S3 and S5).

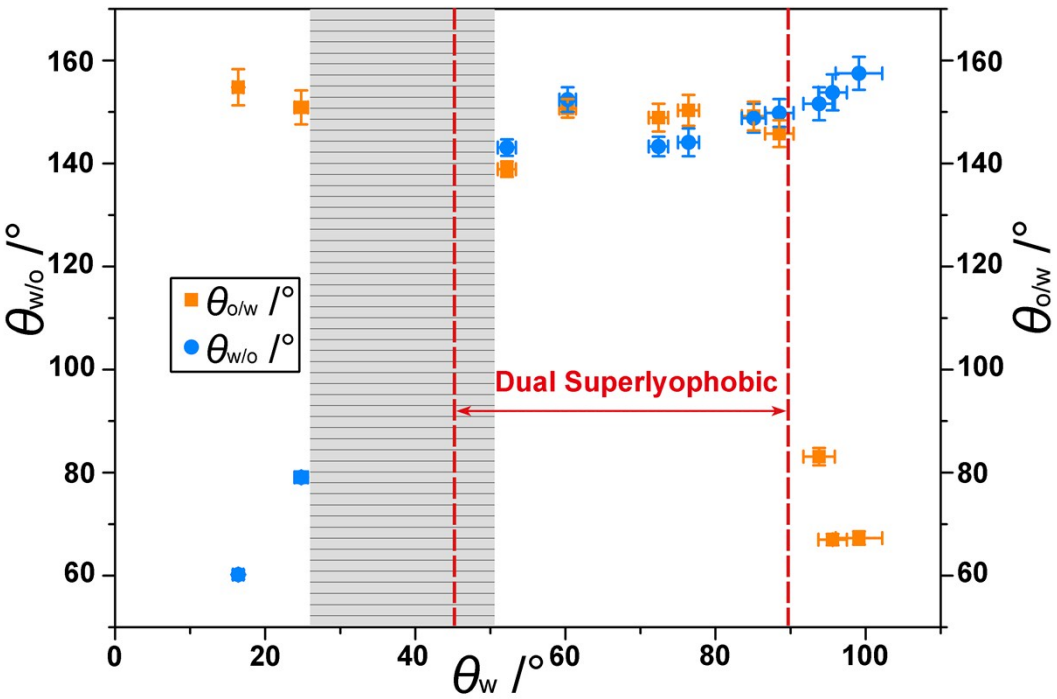


**Figure S10.** The under-liquid wetting behaviors of TFPNMs. In the TCM-water-solid system, the relationship between the $\vartheta_w$ values and the under-liquid wetting behaviors of TFPNMs with different terminal groups, as well as the plasma-treated CTFPNM. The under-liquid wetting behaviors of TFPNMs could be divided into three regions, and the under-liquid dual lyophobic TFPNMs could be obtained with the $\vartheta_w$ ranging from 42.6° to 89.7° (two dotted red lines). The shadow of $\vartheta_w$ ranging from 24.8° to 52.5° is attributed to the lack of suitable experimental modulations of TFPNMs.

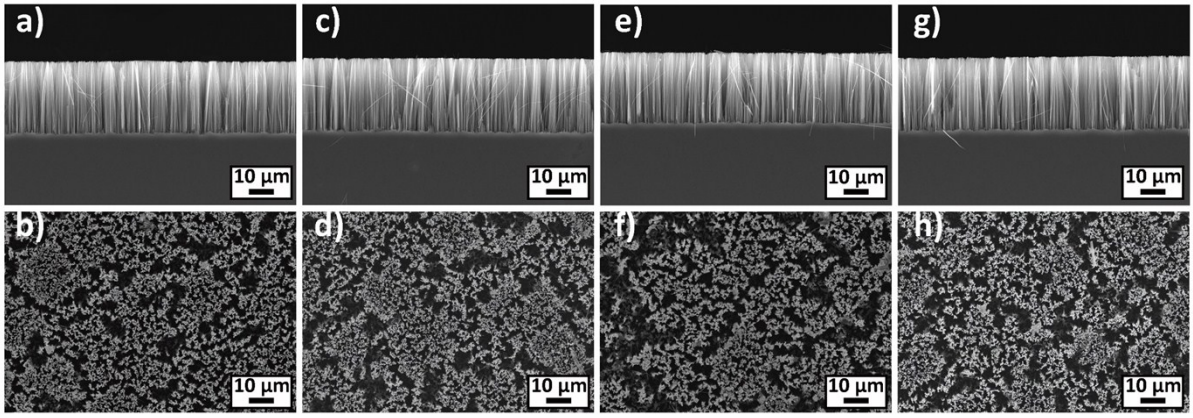


**Figure S11.** SEM images of silicon nanowire arrays (SNWs).[7] a) and b) Initial silicon nanowire array, c) and d) 4-trifluoromethoxy-Ph-terminated SNW, e) and (f) 4-cyan-Ph-terminated SNW, g) and h) 4-carboxyl-Ph-terminated SNWs.

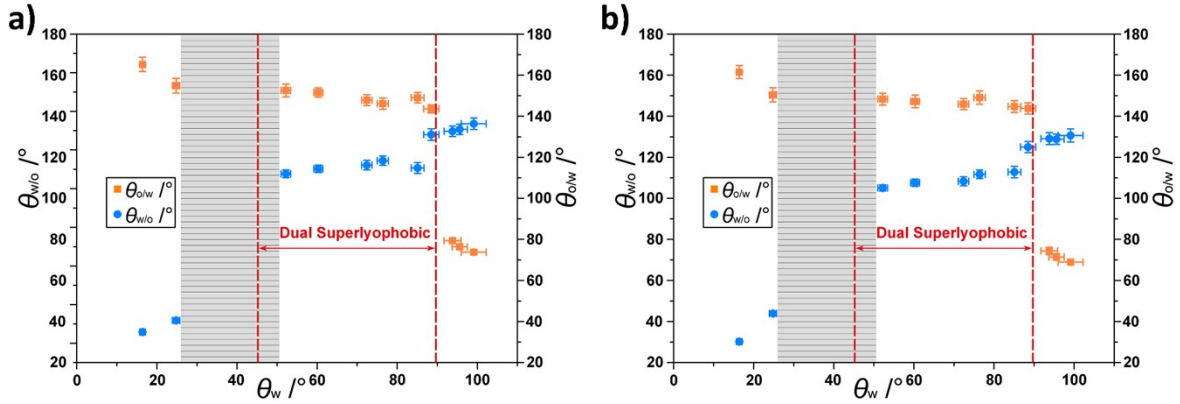


**Figure S12.** The under-liquid wetting behaviors of TF composites coated SNWs (TFSNWs). a) In the CYH-water-solid system and b) in the TCM-water-solid system, the relationship between the $\vartheta_w$ values and the under-liquid wetting behaviors of TFSNWs with different terminal groups, as well as the plasma-treated 4-cyan-Ph-terminated terminated SNW (CTFSNW). The under-liquid wetting behaviors of TF composites coated SNWs could be divided into three regions, in which the under-liquid dual lyophobic surfaces could be obtained with the $\vartheta_w$ ranging from a) 47.3° to 89.1° and b) 42.6° to 89.7° (two dotted red lines), respectively. The shadow of $\vartheta_w$ ranging from 24.8° to 52.5° is attributed to the lack of suitable experimental modulations of TFSNWs.

**Table S1.** Surface groups and the corresponding molecular formula.

| Terminal Groups | Regent | Molecular formula |
|---|---|---|
| 4-Trifluoromethoxy-Ph- | 4-(Trifluoromethoxy)benzonitrile | 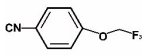 |
| Naphthyl- | 1-Naphthonitrile | 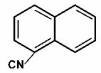 |
| 3-Trifluoromethyl-Ph- | 3-(Trifluoromethyl)benzonitrile | 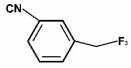 |
| 4-Fluoro-Ph- | 4-Fluorophenylacetonitrile | 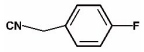 |
| 3-Fluoro-4-hydroxy-Ph- | 3-Fluoro-4-hydroxybenzonitrile | 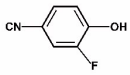 |
| Phenyl- | 3-Phenylpropiononitrile | 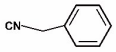 |
| 4-Nitro-Ph- | 4-Nitrobenzonitrile | 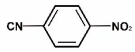 |
| 4-Cyan-Ph- | 1,4-Dicyanobezene | 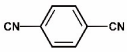 |
| 4-Hydroxy-Ph- | 4-Hydroxybenzonitrile | 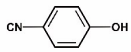 |
| 4-Carboxyl-Ph- | 4-Cyanobenzoic acid | 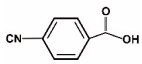 |

**Table S2.** The estimated surface tension of TFPNMs by OWRK method.[a][5]

| TFPNMs | $\gamma_S$ (mJ m$^{-2}$)[b] |
|---|---|
| 4-Trifluoromethoxy-Ph-TFPNM | 25.13 |
| Naphthyl-TFPNM | 25.77 |
| 3-Trifluoromethyl-Ph-TFPNM | 25.95 |
| 4-Fluoro-Ph-TFPNM | 26.42 |
| 3-Fluoro-4-hydroxy-Ph-TFPNM | 26.65 |
| Phenyl-TFPNM | 28.19 |
| 4-Nitro-Ph-TFPNM | 30.12 |
| 4-Cyan-Ph-TFPNM | 39.87 |
| 4-Hydroxy-Ph-TFPNM | 46.61 |
| Plasma-treated CTFPNM | 68.47 |
| 4-Carboxyl-Ph-TFPNM | 72.66 |

[a]Five liquids are used to increase the accuracy of the estimated results about surface tensions: water, ethylene glycol, dimethylformamide, nitromethane and formamide.

[b]$\gamma_S$ represents the estimated result about the surface tension of a certain TFPNM.

**Table S3.** Comparison of the governing relationships with experimental observations in CYH-water-TFPNMs system.

| TFPNMs | Liquid A | Liquid B | $R$ [a] | $\gamma$ [b] | | $\gamma_{AB}$ [c] (mJ m$^{-2}$) | $\vartheta$ [d] | | $\Delta E$ [e] | | Stable ? | |
|---|---|---|---|---|---|---|---|---|---|---|---|---|
| | | | | $\gamma_A$ (mJ m$^{-2}$) | $\gamma_B$ (mJ m$^{-2}$) | | $\vartheta_A$ (°) | $\vartheta_B$ (°) | $\Delta E_1$ (mJ m$^{-2}$) | $\Delta E_2$ (mJ m$^{-2}$) | Theory | Exp |
| 4-Trifluoromethoxy-Ph-TFPNM | $H_2O$ | CYH | 2 | 72.8 | 25.2 | 48.2 | 99.1 | < 5.0 | 25.3 | 121.1 | Y | Y |
| | CYH | $H_2O$ | 2 | 25.2 | 72.8 | 48.2 | < 5.0 | 99.1 | -121.8 | -121.1 | N | N |
| Naphthyl-TFPNM | $H_2O$ | CYH | 2 | 72.8 | 25.2 | 48.2 | 95.6 | < 5.0 | 16.5 | 112.2 | Y | Y |
| | CYH | $H_2O$ | 2 | 25.2 | 72.8 | 48.2 | < 5.0 | 95.6 | -112.9 | -112.2 | N | N |
| 3-Trifluoromethyl-Ph-TFPNM | $H_2O$ | CYH | 2 | 72.8 | 25.2 | 48.2 | 93.8 | < 5.0 | 11.9 | 107.7 | Y | Y |
| | CYH | $H_2O$ | 2 | 25.2 | 72.8 | 48.2 | < 5.0 | 93.8 | -108.4 | -107.7 | N | N |
| 4-Fluoro-Ph-TFPNM | $H_2O$ | CYH | 2 | 72.8 | 25.2 | 48.2 | 88.5 | < 5.0 | -1.6 | 94.2 | Y/N | D L |
| | CYH | $H_2O$ | 2 | 25.2 | 72.8 | 48.2 | < 5.0 | 88.5 | -94.9 | -94.2 | N | D L |
| 3-Fluoro-4-hydroxy-Ph-TFPNM | $H_2O$ | CYH | 2 | 72.8 | 25.2 | 48.2 | 85.1 | < 5.0 | -10.2 | 85.6 | Y/N | D L |
| | CYH | $H_2O$ | 2 | 25.2 | 72.8 | 48.2 | < 5.0 | 85.1 | -86.3 | -85.6 | N | D L |
| Phenyl-TFPNM | $H_2O$ | CYH | 2 | 72.8 | 25.2 | 48.2 | 76.4 | < 5.0 | -32.0 | 63.8 | Y/N | D L |
| | CYH | $H_2O$ | 2 | 25.2 | 72.8 | 48.2 | < 5.0 | 76.4 | -64.5 | -63.8 | N | D L |
| 4-Nitro-Ph-TFPNM | $H_2O$ | CYH | 2 | 72.8 | 25.2 | 48.2 | 72.4 | < 5.0 | -42.5 | 53.3 | Y/N | D L |
| | CYH | $H_2O$ | 2 | 25.2 | 72.8 | 48.2 | < 5.0 | 72.4 | -54.0 | -53.3 | N | D L |
| 4-Cyan-Ph-TFPNM | $H_2O$ | CYH | 2 | 72.8 | 25.2 | 48.2 | 60.3 | < 5.0 | -69.9 | 25.9 | Y/N | D L |
| | CYH | $H_2O$ | 2 | 25.2 | 72.8 | 48.2 | < 5.0 | 60.3 | -26.6 | -25.9 | N | D L |
| 4-Hydroxy-Ph-TFPNM | $H_2O$ | CYH | 2 | 72.8 | 25.2 | 48.2 | 52.2 | < 5.0 | -87.0 | 8.8 | Y/N | D L |
| | CYH | $H_2O$ | 2 | 25.2 | 72.8 | 48.2 | < 5.0 | 52.2 | -9.4 | -8.8 | N | D L |
| Plasma-treated CTFPNM | $H_2O$ | CYH | 2 | 72.8 | 25.2 | 48.2 | 24.8 | < 5.0 | -129.9 | -34.1 | N | N |

| | | | | | | | | | | | | |
|---|---|---|---|---|---|---|---|---|---|---|---|---|
| | CYH | $H_2O$ | 2 | 25.2 | 72.8 | 48.2 | < 5.0 | 24.8 | 33.5 | 34.1 | Y | Y |
| 4-Carboxyl-Ph-TFPNM | $H_2O$ | CYH | 2 | 72.8 | 25.2 | 48.2 | 16.4 | < 5.0 | -137.4 | -41.6 | N | N |
| | CYH | $H_2O$ | 2 | 25.2 | 72.8 | 48.2 | < 5.0 | 16.4 | 41.0 | 41.6 | Y | Y |

[a] $R$ represents the roughness factor of the substrate, which is equal to 2 in this work due to the textured structure of TFPNMs.[6, 7]

[b] $\gamma$ is the surface tension of a certain liquid. $\gamma_A$ and $\gamma_B$ represent the surface tensions of liquid A (liquid to be repelled) and B (infused liquid), respectively (see Table S6).

[c] $\gamma_{AB}$ represents the interfacial tension for liquid A-liquid B interface, which is measured by the pendant droplet method (see Table S7).[8]

[d] $\vartheta$ is the intrinsic contact angle on the smooth surfaces, which are estimated from the measured static contact angles on flat substrates from at least three individual measurements. $\vartheta_A$ and $\vartheta_B$ correspond to liquid A (liquid to be repelled) and B (infused liquid), respectively.

[e] $\Delta E$ represents the total interfacial tension of the wetting models. $\Delta E1$ and $\Delta E2$ refer to the wetting model 1 and wetting model 2, respectively (Figure S9).

Note: "Y" refers to that the liquid B-TFPNM interface is more stable, and liquid B does not get displaced by liquid A from the composite interface; "N" indicates that liquid B-TFPNM interface is not stable enough, and liquid B will be displaced by liquid A; "Y/N" suggests that we cannot identify whether the liquid B can be substituted by liquid A or not, suggesting that the wetting behaviors of these surfaces are conflicting in thermodynamics. "D L" represents the dual lyophobicity of surfaces.

**Table S4.** The under-liquid wetting behaviors of TFPNMs with different terminal groups and plasma-treated TFPNM in TCM-water-solid system.

| TFPNMs | $\vartheta_{TCM/W}$ (°) | $\vartheta_{W/TCM}$ (°) |
|---|---|---|
| 4-Trifluoromethoxy-Ph-TFPNM | 67.3 ± 1.3 | 157.5 ± 3.2 |
| Naphthyl-TFPNM | 67.0 ± 1.1 | 153.8 ± 3.5 |
| 3-Trifluoromethyl-Ph-TFPNM | 83.1 ± 1.7 | 151.6 ± 3.2 |
| 4-Fluoro-Ph-TFPNM | 145.8 ± 2.6 | 149.8 ± 2.7 |
| 3-Fluoro-4-hydroxy-Ph-TFPNM | 149.2 ± 2.8 | 148.8 ± 2.8 |
| Phenyl-TFPNM | 150.3 ± 3.0 | 144.1 ± 2.7 |
| 4-Nitro-Ph-TFPNM | 148.9 ± 2.7 | 143.3 ± 1.9 |
| 4-Cyan-Ph-TFPNM | 150.7 ± 1.8 | 152.4 ± 2.4 |
| 4-Hydroxy-Ph-TFPNM | 138.9 ± 1.5 | 143.1 ± 1.6 |
| Plasma-treated CTFPNM | 150.9 ± 3.3 | 79.1 ± 1.1 |
| 4-Carboxyl-Ph-TFPNM | 154.8 ± 3.5 | 60.2 ± 0.9 |

**Table S5.** Comparison of the governing relationships with experimental observations in TCM-water-TFPNMs system.

| TFPNMs | Liquid A | Liquid B | $R$ [a] | $\gamma$ [b] | | $\gamma_{AB}$ [c] (mJ m$^{-2}$) | $\vartheta$ [d] | | $\Delta E$ [e] | | Stable ? | |
|---|---|---|---|---|---|---|---|---|---|---|---|---|
| | | | | $\gamma_A$ (mJ m$^{-2}$) | $\gamma_B$ (mJ m$^{-2}$) | | $\vartheta_A$ (°) | $\vartheta_B$ (°) | $\Delta E_1$ (mJ m$^{-2}$) | $\Delta E_2$ (mJ m$^{-2}$) | Theory | Exp |
| 4-Trifluoromethoxy-Ph-TFPNM | $H_2O$ | TCM | 2 | 72.8 | 27.0 | 53.2 | 99.1 | < 5.0 | 23.8 | 122.8 | Y | Y |
| | TCM | $H_2O$ | 2 | 27.0 | 72.8 | 53.2 | < 5.0 | 99.1 | -130.2 | -122.8 | N | N |
| Naphthyl-TFPNM | $H_2O$ | TCM | 2 | 72.8 | 27.0 | 53.2 | 95.6 | < 5.0 | 15.0 | 114.0 | Y | Y |
| | TCM | $H_2O$ | 2 | 27.0 | 72.8 | 53.2 | < 5.0 | 95.6 | -121.5 | -114.0 | N | N |
| 3-Trifluoromethyl-Ph-TFPNM | $H_2O$ | TCM | 2 | 72.8 | 27.0 | 53.2 | 93.8 | < 5.0 | 10.5 | 109.5 | Y | Y |
| | TCM | $H_2O$ | 2 | 27.0 | 72.8 | 53.2 | < 5.0 | 93.8 | -116.8 | -109.5 | N | N |
| 4-Fluoro-Ph-TFPNM | $H_2O$ | TCM | 2 | 72.8 | 27.0 | 53.2 | 88.5 | < 5.0 | -3.0 | 96.0 | Y/N | D L |
| | TCM | $H_2O$ | 2 | 27.0 | 72.8 | 53.2 | < 5.0 | 88.5 | -103.4 | -96.0 | N | D L |
| 3-Fluoro-4-hydroxy-Ph-TFPNM | $H_2O$ | TCM | 2 | 72.8 | 27.0 | 53.2 | 85.1 | < 5.0 | -11.6 | 87.4 | Y/N | D L |
| | TCM | $H_2O$ | 2 | 27.0 | 72.8 | 53.2 | < 5.0 | 85.1 | -94.8 | -87.4 | N | D L |
| Phenyl-TFPNM | $H_2O$ | TCM | 2 | 72.8 | 27.0 | 53.2 | 76.4 | < 5.0 | -33.4 | 65.3 | Y/N | D L |
| | TCM | $H_2O$ | 2 | 27.0 | 72.8 | 53.2 | < 5.0 | 76.4 | -73.0 | -65.3 | N | D L |
| 4-Nitro-Ph-TFPNM | $H_2O$ | TCM | 2 | 72.8 | 27.0 | 53.2 | 72.4 | < 5.0 | -43.9 | 55.1 | Y/N | D L |
| | TCM | $H_2O$ | 2 | 27.0 | 72.8 | 53.2 | < 5.0 | 72.4 | -62.4 | -55.1 | N | D L |
| 4-Cyan-Ph-TFPNM | $H_2O$ | TCM | 2 | 72.8 | 27.0 | 53.2 | 60.3 | < 5.0 | -71.3 | 27.7 | Y/N | D L |
| | TCM | $H_2O$ | 2 | 27.0 | 72.8 | 53.2 | < 5.0 | 60.3 | -35.1 | -27.7 | N | D L |
| 4-Hydroxy-Ph-TFPNM | $H_2O$ | TCM | 2 | 72.8 | 27.0 | 53.2 | 52.2 | < 5.0 | -88.4 | 10.6 | Y/N | D L |
| | TCM | $H_2O$ | 2 | 27.0 | 72.8 | 53.2 | < 5.0 | 52.2 | -18.0 | -10.6 | N | D L |
| Plasma-treated CTFPNM | $H_2O$ | TCM | 2 | 72.8 | 27.0 | 53.2 | 24.8 | < 5.0 | -131.4 | -32.4 | N | N |

| | | | | | | | | | | | | |
|---|---|---|---|---|---|---|---|---|---|---|---|---|
| | TCM | $H_2O$ | 2 | 27.0 | 72.8 | 53.2 | < 5.0 | 24.8 | 25.0 | 32.4 | Y | Y |
| 4-Carboxyl-Ph-TFPNM | $H_2O$ | TCM | 2 | 72.8 | 27.0 | 53.2 | 16.4 | < 5.0 | -138.9 | -39.9 | N | N |
| | TCM | $H_2O$ | 2 | 27.0 | 72.8 | 53.2 | < 5.0 | 16.4 | 32.5 | 39.9 | Y | Y |

[a]$R$ represents the roughness factor of the substrate, which is equal to 2 in this work due to the textured structure of TFPNMs.[6, 7]

[b]$\gamma$ is the surface tension of a certain liquid. $\gamma_A$ and $\gamma_B$ represent the surface tensions of liquid A (liquid to be repelled) and B (infused liquid), respectively (see Table S6).

[c]$\gamma_{AB}$ represents the interfacial tension for liquid A-liquid B interface, which is measured by the pendant droplet method (see Table S7).[8]

[d]$\vartheta$ is the intrinsic contact angle on the smooth surfaces, which are estimated from the measured static contact angles on flat substrates from at least three individual measurements. $\vartheta_A$ and $\vartheta_B$ correspond to liquid A (liquid to be repelled) and B (infused liquid), respectively.

[e]$\Delta E$ represents the total interfacial tension of the wetting models. $\Delta E1$ and $\Delta E2$ refer to the wetting model 1 and wetting model 2, respectively (Figure S9).

Note: "Y" refers to that the liquid B-TFPNM interface is more stable, and liquid B does not get displaced by liquid A from the composite interface; "N" indicates that liquid B-TFPNM interface is not stable enough, and liquid B will be displaced by liquid A; "Y/N" suggests that we cannot identify whether the liquid B can be substituted by liquid A or not, suggesting that the wetting behaviors of these surfaces are conflicting in thermodynamics. "D L" represents the dual lyophobicity of surfaces.

**Table S6.** Surface tensions of water and various oils.

| Liquid | Liquid Abv. | Surface Tension ($\gamma$) (mJ m$^{-2}$) |
|---|---|---|
| water | $H_2O$ | 72.8 ± 0.3 |
| cyclohexane | CYH | 25.2 ± 0.2 |
| tetrachloromethane | TCM | 27.0 ± 0.2 |

Note: The surface tensions ($\gamma$) of water, CYH and TCM were performed by the pendant droplet method at ambient conditions (temperature: 23-25°C, relative humidity: 35-38%).

**Table S7.** Interfacial tensions between water and various oils.

| Liquid / Liquid | Surface Tension ($\gamma_{AB}$) (mJ m$^{-2}$) |
|---|---|
| $H_2O$/CYH | 48.2 ± 0.5 |
| $H_2O$/TCM | 53.2 ± 0.7 |

Note: $\gamma_{AB}$ represents the interfacial tension between water and various oils, which is measured by the pendant droplet method at ambient conditions (temperature: 23-25°C).[8]

**Table S8.** The intrinsic water contact angles ($\vartheta_w$) and under-liquid wetting behaviors of TFSNWs with different terminal groups and plasma-treated CTFSNWs in CYH-water-solid system and TCM-water-solid system, respectively.

| TFSNWs | $\vartheta_W$ (°) | $\vartheta_{CYH/W}$ (°) | $\vartheta_{W/CYH}$ (°) | $\vartheta_{TCM/W}$ (°) | $\vartheta_{W/TCM}$ (°) |
|---|---|---|---|---|---|
| 4-Trifluoromethoxy-Ph-TFSNW | 99.1 ± 3.1 | 67.1 ± 1.0 | 133.6 ± 3.0 | 68.9 ± 1.4 | 130.6 ± 3.2 |
| Naphthyl- TFSNW | 95.6 ± 1.9 | 69.9 ± 1.5 | 130.7 ± 2.7 | 71.4 ± 1.6 | 128.8 ± 2.5 |
| 3-Trifluoromethyl-Ph- TFSNW | 93.8 ± 2.1 | 73.1 ± 1.1 | 129.7 ± 2.7 | 74.4 ± 1.8 | 129.1 ± 2.9 |
| 4-Fluoro-Ph- TFSNW | 88.5 ± 1.9 | 141.3 ± 2.1 | 128.0 ± 3.0 | 143.8 ± 2.7 | 125.0 ± 2.7 |
| 3-Fluoro-4-hydroxy-Ph- TFSNW | 85.1 ± 1.6 | 147.1 ± 2.7 | 110.7 ± 2.8 | 144.7 ± 2.9 | 112.8 ± 2.8 |
| Phenyl- TFSNW | 76.4 ± 1.4 | 144.0 ± 2.9 | 114.5 ± 2.4 | 149.1 ± 3.2 | 111.7 ± 2.1 |
| 4-Nitro-Ph- TFSNW | 72.4 ± 1.3 | 145.8 ± 2.8 | 112.2 ± 2.5 | 145.9 ± 2.7 | 108.3 ± 2.2 |
| 4-Cyan-Ph- TFSNW | 60.3 ± 1.1 | 149.8 ± 2.4 | 110.3 ± 1.9 | 147.2 ± 3.1 | 107.6 ± 1.8 |
| 4-Hydroxy-Ph- TFSNW | 52.2 ± 1.2 | 150.8 ± 3.3 | 107.7 ± 2.0 | 148.3 ± 2.9 | 105.1 ± 1.5 |
| Plasma-treated CFSNW | 24.8 ± 0.9 | 153.3 ± 3.8 | 31.8 ± 0.7 | 150.4 ± 3.5 | 43.9 ± 0.9 |
| 4-Carboxyl-Ph- TFSNW | 16.4 ± 0.7 | 164.3 ± 3.7 | 25.8 ± 0.3 | 161.5 ± 3.2 | 30.2 ± 0.7 |

**Table S9.** Comparison of the governing relationships with the reported experimental observations for various liquid-A-liquid-B-solid combinations.[9]

| Coatings | Liquid A | Liquid B | $R^a$ | $\gamma^b$ | | $\gamma_{AB}{}^c$ (mJ m$^{-2}$) | $\vartheta^d$ | | $\Delta E^e$ | | Stable ? | |
|---|---|---|---|---|---|---|---|---|---|---|---|---|
| | | | | $\gamma_A$ (mJ m$^{-2}$) | $\gamma_B$ (mJ m$^{-2}$) | | $\vartheta_A$ (°) | $\vartheta_B$ (°) | $\Delta E_1$ (mJ m$^{-2}$) | $\Delta E_1$ (mJ m$^{-2}$) | Theory | Exp |
| SU8 | $H_2O$ | CYH | 1.36 | 25.2 | 72.8 | 48.2 | 72.0 | < 5.0 | -42.8 | 53.0 | Y/N | D L |
| | CYH | $H_2O$ | 1.36 | 25.2 | 72.8 | 48.2 | < 5.0 | 72.0 | -53.7 | -53.0 | N | D L |
| | $H_2O$ | TCM | 1.36 | 27.0 | 72.8 | 53.2 | 72.0 | < 5.0 | -44.2 | 54.8 | Y/N | D L |
| | TCM | $H_2O$ | 1.36 | 27.0 | 72.8 | 53.2 | < 5.0 | 72.0 | -62.2 | -54.8 | N | D L |
| CPTS | $H_2O$ | CYH | 1.36 | 25.2 | 72.8 | 48.2 | 57.0 | < 5.0 | -77.1 | 18.7 | Y/N | D L |
| | CYH | $H_2O$ | 1.36 | 25.2 | 72.8 | 48.2 | < 5.0 | 57.0 | -19.4 | -18.7 | N | D L |
| | $H_2O$ | TCM | 1.36 | 27.0 | 72.8 | 53.2 | 57.0 | < 5.0 | -78.4 | 20.5 | Y/N | D L |
| | TCM | $H_2O$ | 1.36 | 27.0 | 72.8 | 53.2 | < 5.0 | 57.0 | -27.9 | -20.5 | N | D L |

[a]$R$ represents the roughness factor of the substrate, and is listed in the literature as 1.36.

[b]$\gamma$ is the surface tension of a certain liquid. $\gamma_A$ and $\gamma_B$ represent the surface tensions of liquid A (liquid to be repelled) and B (infused liquid), respectively (see Table S6).

[c]$\gamma_{AB}$ represents the interfacial tension for liquid A-liquid B interface, which is measured by the pendant droplet method (see Table S7).

[d]$\vartheta$ is the intrinsic contact angle on the smooth surfaces. $\vartheta_A$ and $\vartheta_B$ correspond to liquid A (liquid to be repelled) and B (infused liquid), respectively. The values are listed in the literature.

[e]$\Delta E$ represents the total interfacial tension of the wetting models. $\Delta E1$ and $\Delta E2$ refer to the wetting model 1 and wetting model 2, respectively (Figure S9).

Note: "Y" refers to that the liquid B-solid interface is more stable, and liquid B does not get displaced by liquid A from the composite interface; "N" indicates that liquid B-solid interface is not stable enough, and liquid B will be displaced by liquid A; "Y/N" suggests that we cannot identify whether the liquid B can be substituted by liquid A or not, suggesting that the wetting behaviors of these surfaces are conflicting in thermodynamics. "D L" represents

dual lyophobicity of the solid surface.

**References**


1 O. P. Bahl, L. M. Manocha, *Carbon*. 1974, **12**, 417-423.

2 L. Pérez-Manríquez, J. Aburabi'e, P. Neelakanda, K.-V. Peinemann, *React. Funct. Polym.* 2015, **86**, 243-247.

3 X. Shen, J. Dai, Y. Liu, X. Liu, J. Zhu, *Polymer.* 2017, **122**, 258-269.

4 T. D. Lu, B. Z. Chen, J. Wang, T. Z. Jia, X. L. Cao, Y. Wang, W. Xing, C. H. Lau, S. P. Sun, *J. Mater. Chem. A.* 2018, **6**, 15047-15056.

5 Y. Wang, J. Di, L. Wang, X. Li, N. Wang, B. Wang, Y. Tian, L. Jiang, J. Yu, *Nat. Commun.* 2017, **8**, 575;

6 T. S. Wong, S. H. Kang, S. K. Tang, E. J. Smythe, B. D. Hatton, A. Grinthal, J. Aizenberg, *Nature.* 2011, **477**, 443-447.

7 B. Pokroy, A. K. Epstein, M. C. M. Persson-Gulda, J. Aizenberg, *Adv Mater.* 2009, **21**, 463–469.

8 F. M. Fowkes, *Ind. Eng. Chem.* 1964, **56**, 40–52.

9 X. Tian, V. Jokinen, J. Li, J. Sainio, R. H. Ras, *Adv Mater.* 2016, **28**, 10652-10658.